Invited Review
Back to the Future: Ribonuclease A

Garland R. Marshall, Jiawen A. Feng, Daniel J. Kuster
Center for Computational Biology, Department of Biochemistry and Molecular Biophysics, Washington University School of Medicine, St. Louis, MO 63110

Received 27 April 2007; revised 2 August 2007; accepted 9 August 2007
Published online 14 September 2007 in Wiley InterScience (www.interscience.wiley.com). DOI 10.1002/bip.20845

ABSTRACT:

Pancreatic ribonuclease A (EC 3.1.27.5, RNase) is, perhaps, the best-studied enzyme of the 20th century. It was isolated by René Dubos, crystallized by Moses Kunitz, sequenced by Stanford Moore and William Stein, and synthesized in the laboratory of Bruce Merrifield, all at the Rockefeller Institute/University. It has proven to be an excellent model system for many different types of experiments, both as an enzyme and as a well-characterized protein for biophysical studies. Of major significance was the demonstration by Chris Anfinsen at NIH that the primary sequence of RNase encoded the three-dimensional structure of the enzyme. Many other prominent protein chemists/enzymologists have utilized RNase as a dominant theme in their research. In this review, the history of RNase and its offspring, RNase S (S-protein/S-peptide), will be considered, especially the work in the Merrifield group, as a preface to preliminary data and proposed experiments addressing topics of current interest. These include entropy–enthalpy compensation, entropy of ligand binding, the impact of protein modification on thermal stability, and the role of protein dynamics in enzyme action. In continuing to use RNase as a prototypical enzyme, we stand on the shoulders of the giants of protein chemistry to survey the future. © 2007 Wiley Periodicals, Inc. Biopolymers (Pept Sci) 90: 259–277, 2008.

Keywords: ribonuclease A; S-peptide; S-protein; protein dynamics; chimeric enzyme

This article was originally published online as an accepted preprint. The "Published Online" date corresponds to the preprint version. You can request a copy of the preprint by emailing the Biopolymers editorial office at biopolymers@wiley.com

Dedicated to the memory of R. Bruce Merrifield, Nobel Laureate, mentor and friend, and his family, role models all.

Correspondence to: Garland R. Marshall; e-mail: garland@pcg.wustl.edu or garlandm@gmail.com
Contract grant sponsor: NIH
Contract grant number: GM68460
Contract grant sponsor: Computational Biology Training
Contract grant number: GM 008802
Contract grant sponsor: Division of Biology and Biomedical Science at Washington University in St. Louis, Ewing Marion Kauffman Foundation, Department of Biomedical Engineering at Washington University in St. Louis

INTRODUCTION

The vast literature on bovine pancreatic ribonuclease A (EC 3.1.27.5, RNase) was reviewed in 1998[1] by Ronald T. Raines of the University of Wisconsin in which he concluded, "RNase has been the most extensively studied enzyme of the 20th century." While Raines' review emphasized the mechanistic enzymology of RNase, the use of RNase as a model system for protein chemistry and biophysics was also highlighted. Park and Raines[2] have shown that catalysis by RNase is limited by the rate of substrate association, placing RNase in a very select group of highly evolved biological catalysts. Chris Anfinsen of NIH used RNase to demonstrate that its amino acid sequence determined its unique three-dimensional structure.[3] Four Nobel Prizes have been awarded (Anfinsen, Moore, Stein, and Merrifield) for work associated with studies on RNase. Privalov used calorimetric studies of RNase and four other small globular proteins to characterize the highly cooperative nature and thermodynamics of protein folding.[4] Using disulfide-bond chemistry, Scheraga and coworkers[5–9] studied the refolding of RNase. Ribó et al. illustrated the use of pressure to study protein folding/unfolding

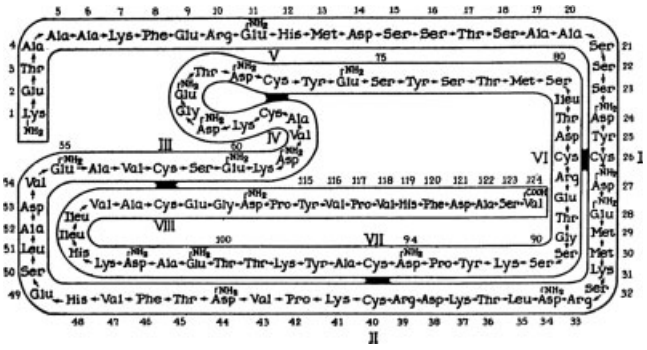

FIGURE 1 Sequence diagram of bovine pancreatic ribonuclease A as determined in the Rockefeller laboratory of Stanford Moore and William Stein. Used with permission from their Nobel Lecture paper in Science (Reproduced from Ref. 11, with permission from AAAS©). Of major significance was the demonstration by Anfinsen with whom Moore and Stein shared the Nobel Prize that the primary sequence of RNase encoded the three-dimensional structure of the enzyme.

with RNase and its mutants as a model system.[10] As RNase contains four disulfide bonds (Figure 1) as well as two *cis*-amide bonds, its folding has been a topic of considerable interest.

In this more personal review, the emphasis is on the historical relation between RNase, the Rockefeller Institute/University, and its influence on R. Bruce Merrifield and his students. In addition, both current and potential future uses of RNase to address fundamental problems in the thermodynamics driving molecular recognition and the dynamics of enzyme catalysis will be highlighted.

RIBONUCLEASE AS MODEL SYSTEM

Bovine Pancreatic Ribonuclease A—Best-Studied Enzyme of the 20th Century and Possibly of the 21st Century as Well

RNase was isolated by René Dubos in 1938,[12] crystallized by Moses Kunitz in 1940,[13] sequenced (Figure 1) by Stanford Moore and William Stein in 1963[14] (with considerable assistance by the Anfinsen group at NIH[15] as well[16]), and synthesized in the Merrifield lab in 1969,[17,18] all at the Rockefeller Institute/University. While GRM was a graduate student in the Merrifield lab (1962–1966), Professors Dubos, Kunitz, Moore, and Stein were still daily participants in lunches at long tables held in the Faculty Lunchroom at Rockefeller, where graduate students could mingle with these legends of protein chemistry. Bruce devoted significant effort to using RNase and its fragments as a testbed for solid phase synthesis, as well as a means of understanding the binding and recognition of peptides by proteins in well-characterized systems. He discussed his fascination with RNase as a model system for examining protein structure and enzymatic activity in his autobiography.[19] Two of the best-characterized protein assembly systems that generate enzymatic activity on complex formation are the S-protein/S-peptide and C-terminal peptide/RNase complexes, the latter being discovered in the Merrifield and Moore labs.

Ribonuclease S and S-Peptide

Fred Richards discovered that RNase (124 residues) could be cleaved by the proteolytic enzyme subtilisin between residues 20 and 21, to yield a fully active complex of RNase S (S-protein, residues 21–124 with S-peptide, residues 1–20), as illustrated in Figure 2.[23,24] Dissociation of the complex eliminated ribonuclease activity, and activity was fully restored when the two components were remixed. Wyckoff and Richards[25,26] determined the three-dimensional structure of RNase S to compare with that of intact RNase A. S-peptide/S-protein (Figure 2) has proven to be an ideal model system for exploring the thermodynamics and molecular recognition requirements for a peptide by a protein-binding site.[27] Based on syntheses and structure–activity studies of S-peptide analogs, Finn and Hofmann[28] suggested that RNase S may be the prototype for peptide–hormone activation of receptors by completion of an active site of an enzyme. The structure of a dimer of RNase in which two N-terminal helical domains are swapped in analogy with the S-peptide interaction has also been determined.[29] A hexapeptide antagonist, YNFEVL, of S-peptide, which has comparable affinity for

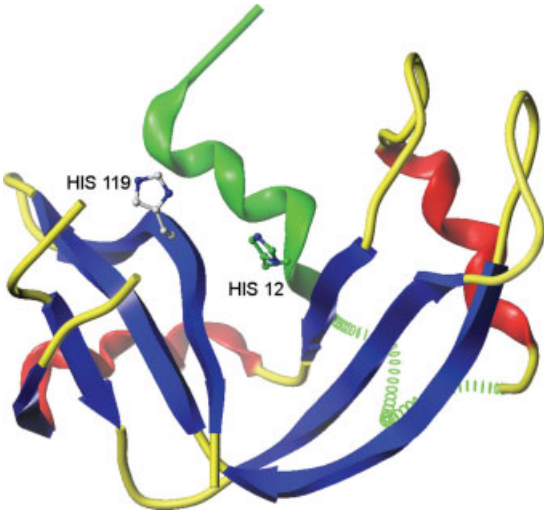

FIGURE 2 Ribbon diagram of RNase S with active-site histidines (12 and 119) shown. S-peptide highlighted as green ribbon; S-protein highlighted as blue (sheets), helices (red) and turns (yellow). Green spring represent unstructured segment in RNase S that is structured in RNase A. Structural data from PDB entry 1DY5.

RNase S-protein, has been discovered utilizing phage display and panning with S-protein.[30]

Further studies have shown that the full-length S-peptide is not required when recombined with S-protein, as the first 14 residues RNase (1–14) alone were able to restore full enzymatic activity.[28] Additionally, nuclear magnetic resonance (NMR) studies have shown the S-peptide to adopt a predominantly disordered state in solution and a helical state when bound to S-protein,[31–33] as shown in the crystal structure of the complex. Simplified analogs of 1–15, AEAAAAKFARAHMAA (as compared to the native 1–15 sequence (S15) KETAAAKFERQHMDS), in which residues not contacting S-protein are converted to alanine, led to active complexes with RNase.[34–36] This fact lends further support to the idea that an α-helical arrangement of residues has functional significance[35] and provides a roadmap to possible introduction of constrained amino acids such as aminoisobutyric acid (Aib). The φ,ψ backbone torsion angles from crystal structures of the S-peptide when complexed with S-protein are plotted in Figure 3. While residues 4–10 have precisely α-helical torsion angles, residues Gln11 and His12 do not.

Variation in binding affinities suggests that understanding and separation of variables in binding thermodynamics is not trivial. Calorimetric studies of the RNase S/S-peptide system are extensive.[40–43] Ratnaparkhi et al.[44] introduced an Aib residue to replace Ala4 in shortened S-peptide (Ala4Aib S16) and compared its binding thermodynamics with S16 (S15 with a C-terminal glycine replacing the carboxamide) using isothermal titration calorimetry (ITC). The more rigid Aib-containing peptide has slightly less affinity than S16 at all temperatures investigated and did not impact the melting temperature of the complex with S-protein. This suggests that initial melting may involve another subdomain of RNase, rather than the S-peptide. The crystal structure of the Aib-containing S16 and enzymatic activity of the complex were "essentially" (authors' comment) identical to that of the S15 complex. At room temperature, neither Ala4Aib nor S16 contained detectable amounts of helix by CD, suggesting that the single Ala4Aib did not induce any helical preference under the conditions examined. While the ΔS of binding is more positive for Ala4Aib, the ΔH for binding is also more positive, and, thus, the system displays entropy/enthalpy compensation. The positive value of $\Delta\Delta H$ was unexpected and possibly due to favorable interactions formed in uncomplexed Ala4Aib. Obviously, these data challenged the basic assumption being tested: that preorganization of the helical backbone will reduce the change in entropy of binding, and that this change will be reflected in enhanced affinity. This makes the RNase S system particularly attractive as a model system for further investigation of the details of binding thermodynamics to resolve this conflict. Nevertheless, examples exist of helical peptides containing Aib residues with nanomolar binding affinities and relatively small sizes in other less well-defined systems. What factors are necessary for preorganization to translate the anticipated loss in entropy of binding to affinity? How complementary do the interacting surfaces need to be? A minor mismatch in steric complementarity can obviously be catastrophic.

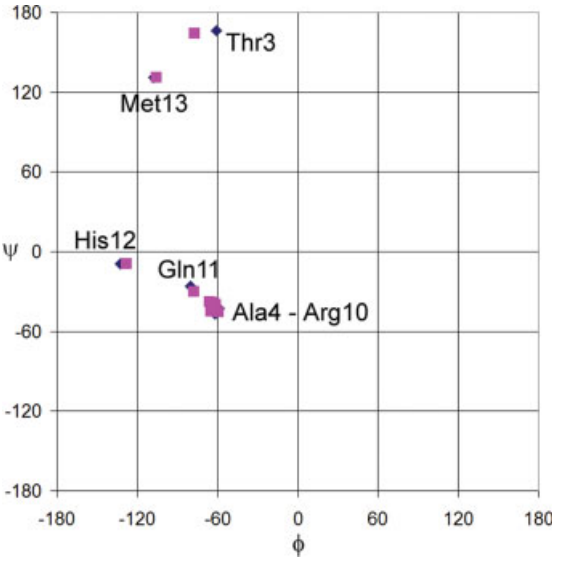

FIGURE 3 Ramachandran (φ,ψ) plot for residues Thr3-Arg10 from RNase S peptide, PDB entry 1DY5 (solved to 0.87 Å; two molecules per asymmetric unit); structural annotation gives Thr3-Met13 as helical for both molecules. The cluster of residues Ala4-Arg10 occurs near "ideal" α-helical values ($\varphi = -57$, $\psi = -47$). Gln11 (near ideal 3_{10}-helical values), Thr3, and His12 deviate from the cluster. Met13 is the dominant side chain in binding affinity[20,21,22] and His12 is essential for catalysis.

Complex of RNase With C-Terminal Segments

Merrifield described a tea conversation he had with T. P. King and Bill Konigsberg, two contemporary protein chemists, at Rockefeller in 1965 in his autobiography.[19] The discussion centered on generating a construct similar to RNase S, but which explored the role of the C-terminal segment of RNase contributing His119 to the catalytic site. Ultimately, the semisynthetic ribonuclease, RNase-(1–118)-(111–124), was evolved to study the role of the C-terminal segment in recognition and catalysis.[45–48] A three-component system, combining equimolar amounts of RNase fragments 1–20, 21–118, and 111–124, retained 30% of the enzymatic activity of intact RNase.[19] Possible utilization of this three-component system in studies of chimeric RNase and preorganization are attractive.

RNase and RNase S Domain-Swapped Dimers

Domain swapping occurs when two monomers exchange structural motifs, α-helix, β-strands or even larger subdomains, to form dimers or higher oligomers and retain the structure of the swapped domains. RNase was the first protein that demonstrated the three-dimensional domain swapping, as shown in the Moore and Stein laboratory.[49] Subsequent work has shown that RNase can form a variety of dimers, trimers, and higher oligomers by swapping the N-terminal α-helix, the C-terminal β-strand, or both, as recently reviewed.[50] The amyloid-like structure seen in the C-terminal dimer of RNase led Eisenberg and coworkers to a general proposal for amyloid formation via domain swapping.[51] Lopez-Alonso et al.[52] have shown that RNase S can also form a dimer analogous to the C-dimer of RNase whose dissociation is strongly slowed by excess S-peptide, suggesting that S-peptide release is rate limiting.

The RNase A Superfamily

A number of enzymes with homology, both in sequence and function to pancreatic RNase A, have been characterized as reviewed by Dyer and Rosenberg.[53] All eight human ribonuclease A-like genes are located on chromosome 14, each encoding a secretory signal sequence with an invariant catalytic triad of two histidines located at each end of the protein and one lysine within a conserved motif (CKXXNTF). Only one, angiogenin/RNase 5, has three disulfide bonds, perhaps representing the ancestral gene of what is thought to be the sole vertebrate-specific enzyme[54]; the others contain the four disulfides seen in RNase itself (Figure 1), although the location of disulfide 65–72 in RNase has been shifted in onconase. Modifications of their respective sequences are thought to be involved with a diversity of functions in host defense against viral and bacterial pathogens.

Peptide Antagonist of S-Protein (YNFEVL)[55]

From a phage library displaying hexapeptides, clones that bound S-protein were selected. Bound peptides showed a sequence motif, (F/Y)NF(E/V)(I/V)(L/V), that bore little resemblance to S-peptide. YNFEVL was synthesized and shown by ITC to bind S-protein with a K_d of 5.5 mM at 25°C, comparable to those reported for some S-peptide variants. The YNFEVL peptide was an antagonist of S-peptide. It did not generate RNAse activity upon binding to S-protein, but blocked the ability of S-peptide to restore enzyme activity by competition. The hexapeptide is considerably smaller than S15 or S-peptide and could provide insight into different binding interactions, as well as possible interaction of the S-peptide with the RNA substrate. To our knowledge, the structure of the complex of YNFELV with S-protein has not been determined.

Intracellular Inhibitors of RNase

Ribonuclease has demonstrated potential in oncology. Within the cell, RNase is complexed with an inhibitory protein (RI).[56] When the surface of RNase is mutated to eliminate recognition by the cytosolic inhibitor (RI), the modified RNase is toxic to cancer cells by degradation of intracellular RNA.[57] These observations provide another opportunity for development of helix mimetics of S-peptide as potential therapeutics. The interaction between RNase and RI is very tight (femtomolar K_d, estimated binding energy = 73.3 kJ mol^{-1}; Ref. 58), and the residue/residue basis of interaction has been mapped by Rutkoski et al.[57] The crystal structure of RNase complexed with RI has been determined (Figure 4) and the role of individual residues of the S-peptide domain to binding affinity examined.[58] Two basic residues of the S-peptide, Lys1 and Lys7, dominate the interaction. Replacement of Lys1 by alanine decreased affinity by 4 kJ mol^{-1}, whereas replacement of Lys7 with alanine reduced affinity by 10 kJ mol^{-1}. Loss in binding energy (16 kJ mol^{-1}) by a double mutation was comparable to RI binding to S-protein alone.[58] Smith and Raines[59] have developed a creative expression system in an *E. coli* strain in which the reductive intracellular environment has been eliminated to allow nascent RNase to form its disulfide bonds and generate enzymatic activity. Mutations within this *E. coli* strain allowed the interface between RNase and RI to be mapped.

HELIX MIMETICS IN MOLECULAR RECOGNITION OF RNASE S

Helical Peptidomimetics

Design and syntheses of a variety of scaffolds, primarily polyaromatic, to orient amino acid side chains and mimic the recognition surface of peptide helices has been reviewed by Che et al.[60] S-peptide is an excellent model for exploring surface complementarity and the thermodynamics of S-protein recognition. Because the S-peptide contributes His12 to complete the active site of RNase S, helix mimetics may be designed to bind to S-protein and regenerate enzymatic activity. Binding of a helix mimetic to S-protein could be detected by a number of techniques, including competition with a fluorescently labeled S-peptide, ITC, etc. Yet, to determine that the correct (i.e., "designed") alignment of the two components in the RNase S complex occurred would require structural studies by crystallography or NMR. The requirement for catalysis of precise positioning of the catalytic His12 residue, however, effectively couples a thermodynamically driven binding event to a simple enzymatic assay. Deciding what exact variations in helix geometry to target with a helix mimetic of S-peptide is nontrivial as discussed below.

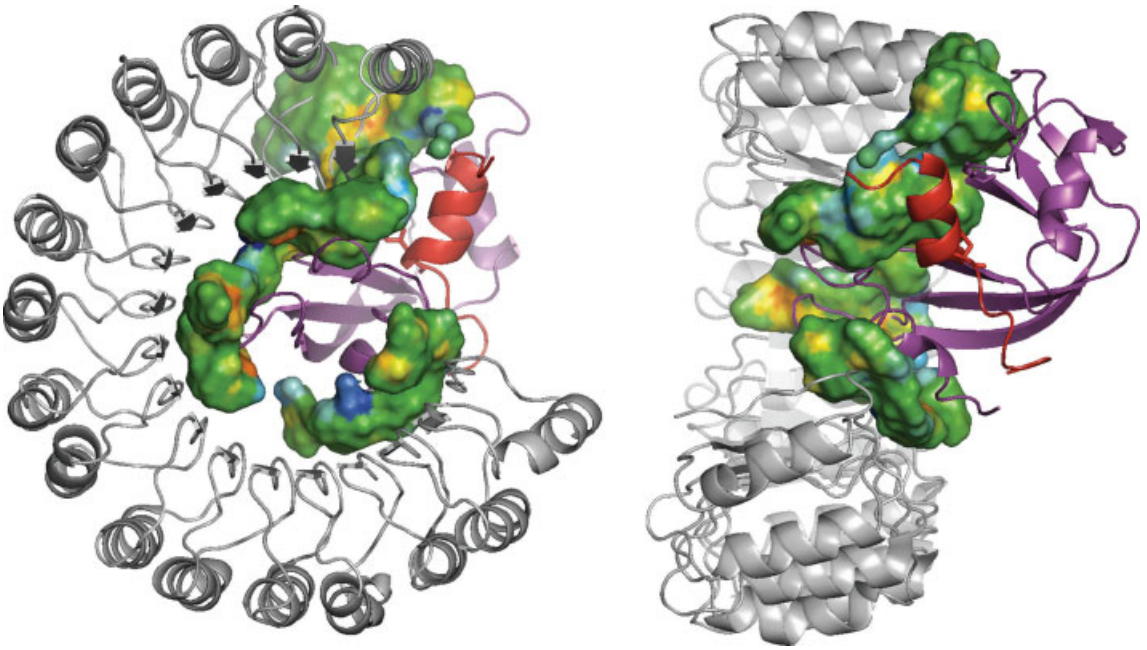

FIGURE 4 Orthogonal views of complex between RNase and its intracellular inhibitor (RI).[37,38] The S-peptide segment is highlighted in red, helices and sheets of leucine-rich domains of RI in gray, and rest of RNase A in magenta ribbon diagrams. The filled sections of the inhibitor are those residues that FADE[39] selected for significant surface contact with RNase.

Helical Parameters

The prevailing viewpoint is that the classical α-helix ($\varphi = -57^\circ$, $\psi = -47^\circ$) with a 13-member hydrogen-bonding scheme predominates in protein crystal structures. Further investigation challenges this tacit assumption and the frequently incorrect assignment of classic α-helicity for many helical subdomains in the PDB, including the S-peptide. A Ramachandran (φ,ψ) plot of atomic resolution crystal data for RNase S-peptide (two molecules per asymmetric unit) in Figure 3 shows that not all helical residues are precisely α-helical. Forcing the side chains of residues 11 and 12, however, to orient on a "perfect" α-helical scaffold would misalign the histidine side chain and disrupt catalytic activity. Further, this would also misalign the methionine-13 side chain that has been shown to be the "hot spot" in the S-peptide for binding affinity.[20,42] A recent examination of over 900 helical residues in high-resolution crystal structures of proteins indicated that the experimentally observed distribution (Figure 5) is skewed from the classic α-helix, toward the region of the 3_{10} helix, suggesting a predominance of bifurcated hydrogen-bonding schemes.[61] This view is supported by molecular dynamics (MD) simulations of crambin (58 residues) in explicit solvent using the next-generation AMOEBA force field,[62] followed by analysis of helical length (Figure 6). Most helical-mimetic scaffolds proposed to date do not possess backbone flexibility that would allow for induced fit upon binding a protein. Rather

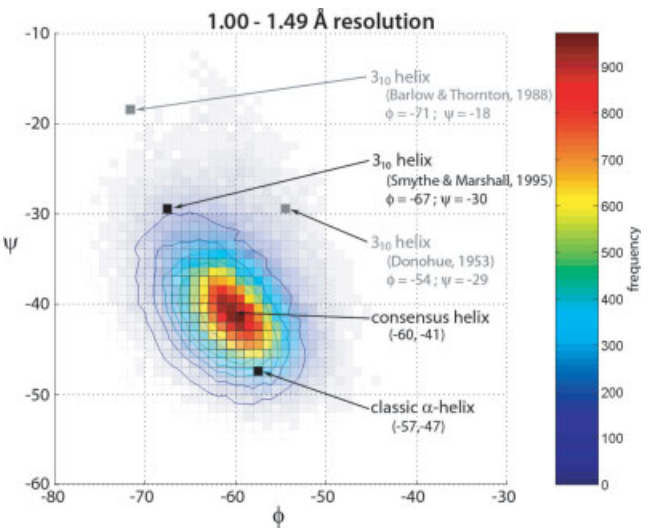

FIGURE 5 Frequency and distribution of peptide backbone torsion angles (φ,ψ) for over 5 million residues in crystal structures with 1.0–1.49 Å resolution. The maximum population for helical residues occurs at ($\varphi = -60$, $\psi = -41$) rather than the classical α-helical definition of ($\varphi = -57$, $\psi = -47$). (φ,ψ) pair values were calculated by analyzing the structures of peptide planes in the PDB, assigning hydrogen bonds and detecting helices by $i \rightarrow i + 3$ and $i \rightarrow i + 4$ hydrogen-bonding patterns. Values are strictly implied from high-resolution structures and are not biased by any secondary structure predictions.

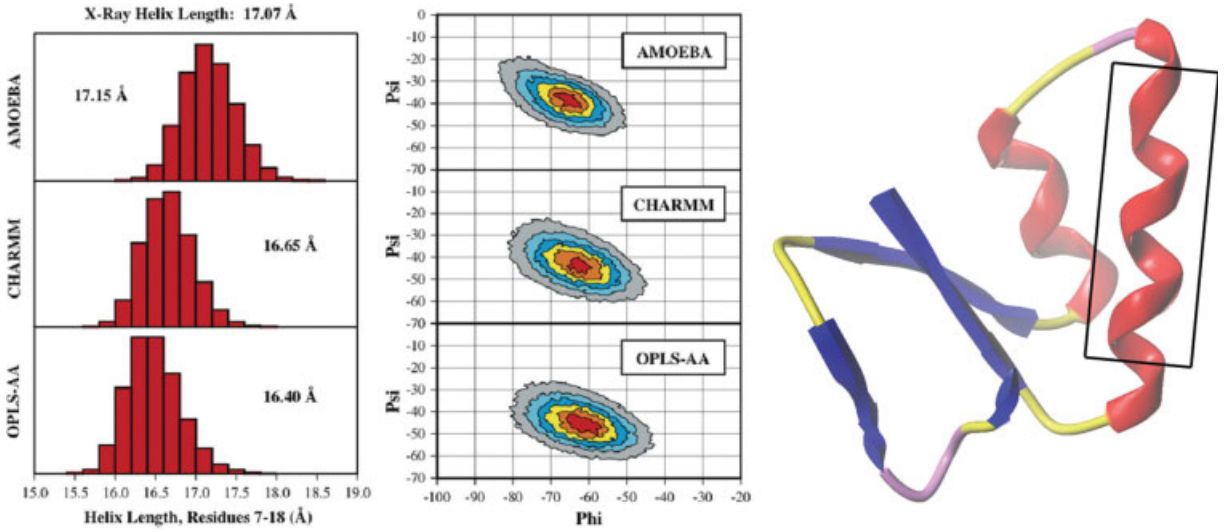

FIGURE 6 Length of helical residues 7–18 of crambin (46 residues, PDB = 1EJG, resolution = 0.54 Å) after long molecular dynamics (MD) simulations in explicit water. Results using three different force fields: AMOEBA – helix agrees better with experimental X-ray data, minimum shifted toward 3_{10}-helix; CHARMM and OPLS-AA – helix were significantly shorter than experimental values, minimum were much closer to classical helical values.

most scaffolds have been designed against ideal or single-case α-helices and, thus, will not generically complement other helix-recognition sites.

α-Methyl Amino Acids

Marshall and Bosshard[63] first published the dramatic effect on helical propensity of replacing the α-proton of an amino acid with a methyl group in 1972. Examination of the reproduced Ramachandran plots (Figure 7) from this paper showed the differences in allowed regions of the two variables, φ and ψ, for the capped amino acid, acetyl-L-alanine *N*-methylamide (Figure 7A) and acetyl-D-alanine *N*-methylamide (Figure 7E). Replacement of a hydrogen with a methyl group on the peptide backbone results in significant loss in possible values for φ and ψ; for example, the impact of a methyl replacement for the amide hydrogen is shown in two plots, the first for acetyl-*N*-methyl-L-alanine *N*-methylamide, which restricts φ (Figure 7B), and the second for acetyl-D-alanine *N*-methylamide which restricts ψ (Figure 7C). These plots indicate why proline, or any other *N*-methyl amino acid, has difficulties being accommodated within the helical segments of proteins. The most dramatic change was seen, however, when the α-hydrogen of the alanine was replaced by a methyl group, acetyl-L-aminoisobutyric *N*-methylamide (Figure 7D), simultaneously restricting both φ and ψ. This prediction that α-methyl amino acids would restrict the flexibility of the peptide backbone to only those regions of φ,ψ space common to both acetyl-L-alanine *N*-methylamide (Figure 7A) and acetyl-D-alanine *N*-methylamide (Figure 7E) has been confirmed subsequently by numerous experimental/theoretical studies by the Marshall,[65–69] Karle,[70,71] Toniolo,[72,73] Balaram,[70] and Millhauser[74] groups. By focusing the minimal energy states of the peptide backbone to φ,ψ space associated with right- or left-handed helices, substitutions with α-methyl amino acids preorganize the peptide

FIGURE 7 Ramachandran (φ,ψ) plot for a series of "capped" alanine analogs designed to probe conformational limits imposed by H → CH_3 modifications. (A) Acetyl-L-alanine *N*-methylamide; (B) acetyl-*N*-methyl-L-alanine *N*-methylamide; (C) acetyl-L-alanine *N,N*-dimethylamide; (D) acetyl-aminoisobutyric *N*-methylamide; (E) acetyl-D-alanine *N*-methylamide. Figures (A–D) were recreated from original figures published in 1972 by Marshall and Bosshard.[63] Potential energies of analogs were sampled at 10° increments over (φ,ψ) space using MacroModel 9.1, with minimization at each grid point, using OPLS 2005 force field, GB/SA implicit water solvation and a dielectric constant of 1.5. Contours indicate potential from the minimum, in increments of 0.5 kcal mol^{-1} to a limit of 5 kcal mol^{-1}. Note that the Aib analog, shown in (D), is similar to the intersection of the L-alanine and D-alanine results, shown in (A) and (E), respectively. Similar plots for L-alanine (Figure 6) and L-alanine preceding a proline residue (Figure 13) were previously published by Flory in Chapter VII of his textbook "Statistical Mechanics of Chain Molecules" in 1969.[64]

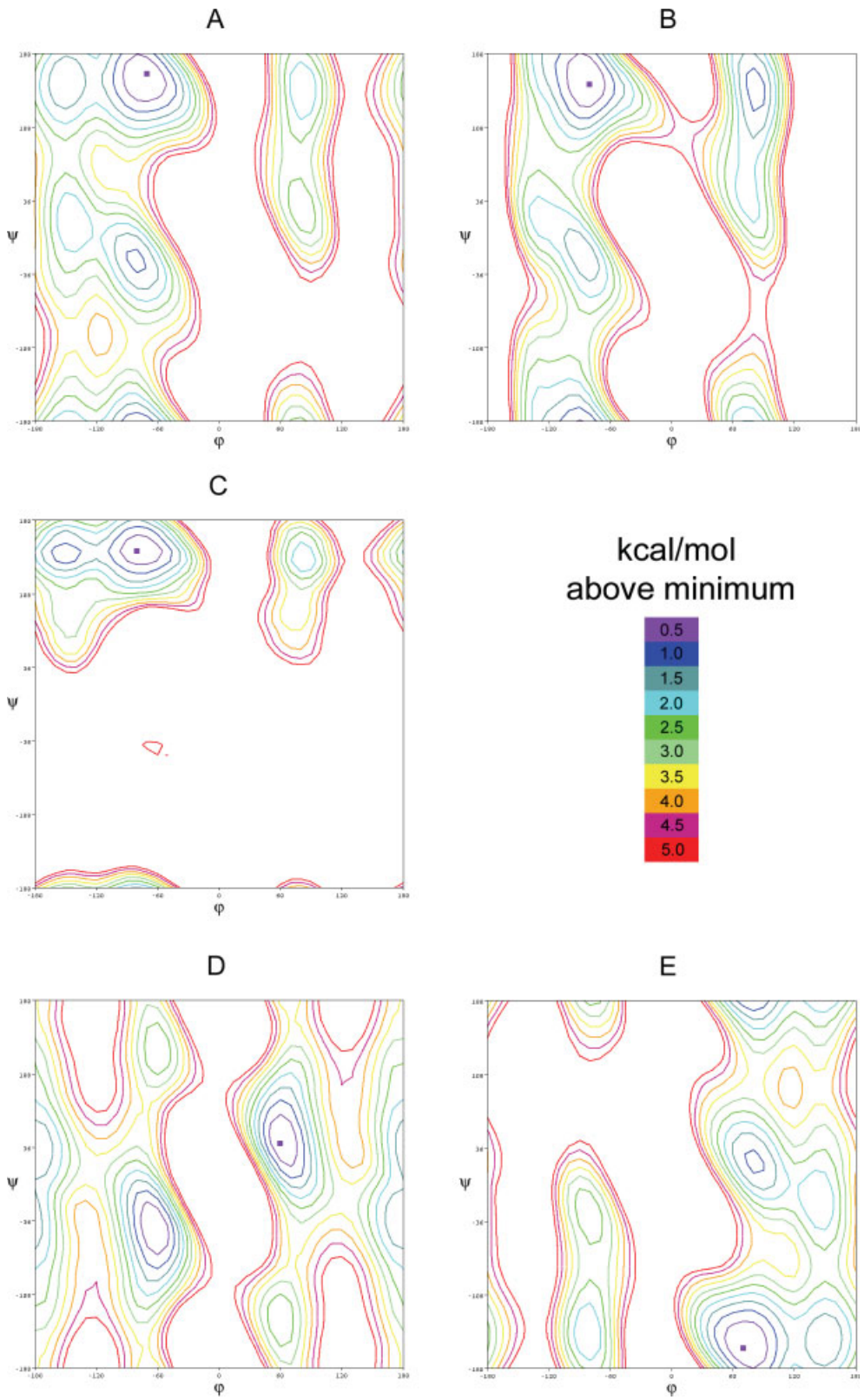

FIGURE 7

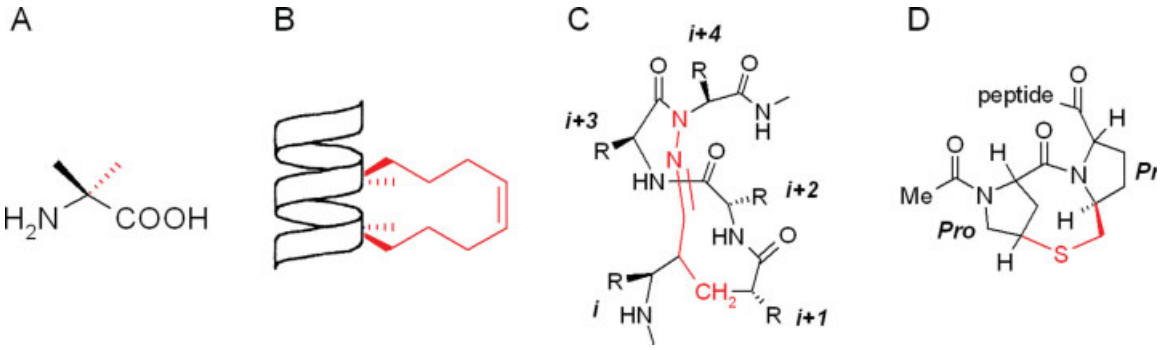

FIGURE 8 Various strategies for stabilizing helices in peptides.[60] (A) α,α-Disubstituted amino acids; (B) side-chain crosslinked peptides; (C) intrachain H-bond surrogates; (D) end-capping templates. Stapling involves a combination of (A) and (B) at the same residues.

to turn or helical conformations at those residues and reduce the entropy of folding/binding. α-Methyl amino acids have become a standard tool in the peptide chemists' repertoire for inducing turns and stabilizing helices.[75] The only negative aspect of their use is the ambiguity regarding which type (α- helix, 3_{10}-helix, or a mixture of the two) of helix is being recognized upon binding.[65] The ability to form rigidified complementary helical surfaces by subtle changes in backbone torsional angles may, in fact, turn out to be a compelling argument for the use of oligomers of α-methyl amino acids as generalized helical mimetics.

Replacing two residues in a sequence with α,α-disubstituted amino acid containing both an α-methyl group and an α-vinyl group followed by olefin metastasis allows rigidification of the helical structure through cyclization of the side chains by "hydrocarbon stapling." A stapled BH3 helix that activated apoptosis was reported by Walensky et al.[76] Alternatively, a similar cyclic stabilization is obtained with side-chain lactam[77] or disulfide formation.[78] Shepherd et al.[79] reported synthesis of a 13-residue helical peptide stabilized by two side-chain lactam bridges that inhibited RSV fusion with an IC_{50} of 36 nM. Multiple strategies for stabilizing helices have been developed and are illustrated in Figure 8. These approaches should be explored as additional ways to stabilize α-methyl oligomers in either the α- or 3_{10}-helical conformations, or perhaps, trap a peptide in the intermediate state with bifurcated hydrogen bonds.

Entropy/Enthalpy Compensation

Enthalpy/entropy compensation remains one of the most difficult aspects of molecular recognition to quantify. It seems intuitively obvious that a tightly binding ligand with high surface complementarity and enhanced enthalpy of binding should bind tighter and be more constrained at the binding site, thus reducing its entropy. It is common to observe a change in the relative contribution of enthalpy and entropy of binding as a set of ligands are examined. As the simplest example of preorganization, incorporation of aminoisobutyric acid (Aib, α-methylalanine) into peptides/proteins restricts the φ and ψ backbone angles adjacent to Aib to those associated with helix formation (Figure 7).[63,65] The Marshall lab utilized this observation to investigate the receptor-bound conformation of several peptides binding to GPCRs.[80–83] By restriction of the adjacent dihedral torsions, insertion of an Aib should also lower the entropic penalty of turn/helix formation upon protein folding, due to preorganization. In a study of the thermodynamics of S-peptide/S-protein complex formation in which α-methylalanine, or aminoisobutyric acid (Aib), had been substituted for Ala4 in the S-peptide by Ratnaparkhi et al. using ITC,[84] the following conclusion was drawn,[44] "The surprising lack of temperature dependence of ΔG_o for Ala4Aib is likely to be due, in part, to the reduced conformational entropy of the uncomplexed peptide as a result of introduction of the Aib residue." Also, it was noted that while the Ala4Aib substitution reduces conformational entropy, $T\Delta S$ compensation is difficult to dissect into its component parts. "Although Aib reduces conformational entropy of the unbound state, there is no increase in protein stability, because of significant enthalpy-entropy compensation."[44] This is exactly the sort of observation that needs detailed analysis by both modern experimental and computational approaches to dissect the fundamentals of these observations.[85]

Combinatorial Library of Helix Mimetics

Bourne et al. (Phenyl-pyridine-based a-helical mimetics: Targeting the CheY-FliM binding site, In preparation) have developed a protocol for synthesis of substituted phenyldipyridyl libraries to serve as helix mimetics (Figure 9). The choice of the phenyldipyridyl scaffold over the diphenyl, terphenyl, and other scaffolds suggested by Jacoby,[86] Hamilton and coworkers,[87–90] and others[91] was based on extensive Density Functional Theory analyses of candidate scaffolds (Figure 10) by Che et al.[60] This study provided an understanding for the design of helix mimetics, and why the simple concept of moving the side chains from the interacting surface of a peptide helix to the aromatic scaffold is not straightforward (Figure 11).

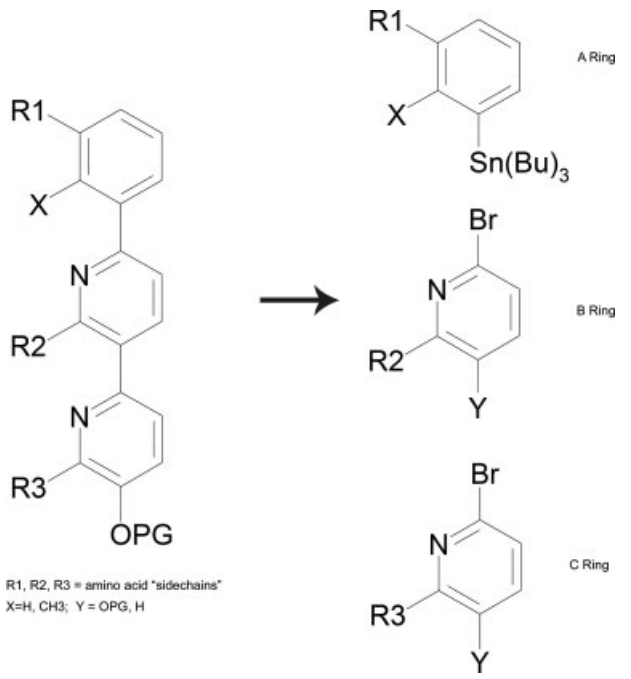

FIGURE 9 Retrosynthetic schematic of combinatorial synthesis of phenyldipyridyl helix mimetics developed in the Marshall lab by Dr. Gregory T. Bourne.

REVERSE TURNS IN RIBONUCLEASE AND BEYOND

Expressed Protein Ligation

Expressed protein ligation (EPL) depends on the use of inteins, bacterial cysteine–protease domains, which can catalyze their own excision from a protein sequence while splicing the N- and C-terminal segments together.[97] By using a mutated intein, the enzyme mechanism can be trapped with the N-terminal sequence as the intein-bound thioester. This activates the unprotected N-terminal segment for chemical ligation to an N-terminal cysteine C-terminal segment. Generation of hybrid proteins with expressed protein domains ligated to synthetic peptide or organic component (Figure 12) is readily accomplished. This approach has provided an ability to combine segments of protein labeled differentially to facilitate biophysical studies.[98–100] Three examples of EPL to generate hybrid constructs of RNase have appeared; two of which probe the role of preorganization on thermal stability and enzyme catalysis. In 1998, Evans et al.[101] produced RNase A by expressing an inactive truncated form, the first 109 amino acids of RNase A, as a fusion protein consisting of RNase 1–109, an intein, and a chitin-binding domain. Thiol-induced cleavage of the precursor fusion protein led to the liberation of RNase 1–109 with a C-terminal thioester. Addition of synthetic peptides representing residues 110–124 led to the generation of full-length products with catalytic activity indicative of wild-type RNase. The turnover numbers and K_m for ligated and renatured RNase A were 8.2 s^{-1} and 1.5 mM, which are in good agreement with reported values of 8.3 s^{-1} and 1.2 mM.[48] Arnold et al.[102] also used EPL to prepare semisynthetic RNase, essentially indistinguishable from the wild-type enzyme.

Impact of Reverse-Turn Mimetics on Protein Stability

Reverse-turn mimetics[103] have been constructed from such diverse structural approaches as cyclically constrained pepti-

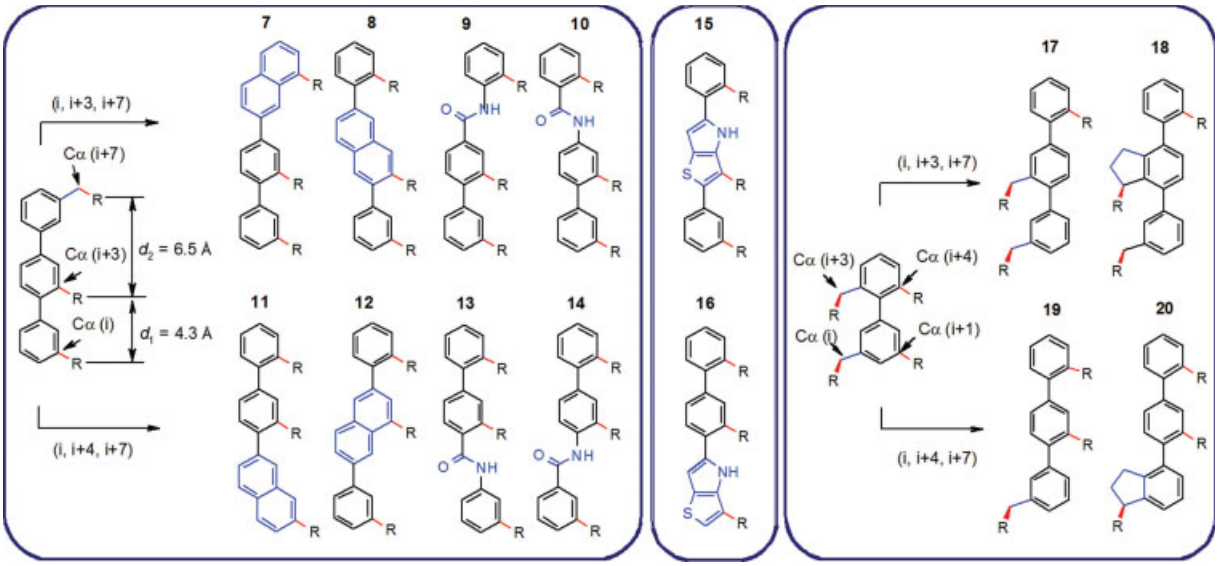

FIGURE 10 Structures examined by Che et al.[60] as candidate organic scaffolds to position amino acid side chains to mimic the surfaces of helices, stimulated by the studies of Jacoby[86] and Hamilton and coworkers.[87,88,92–95]

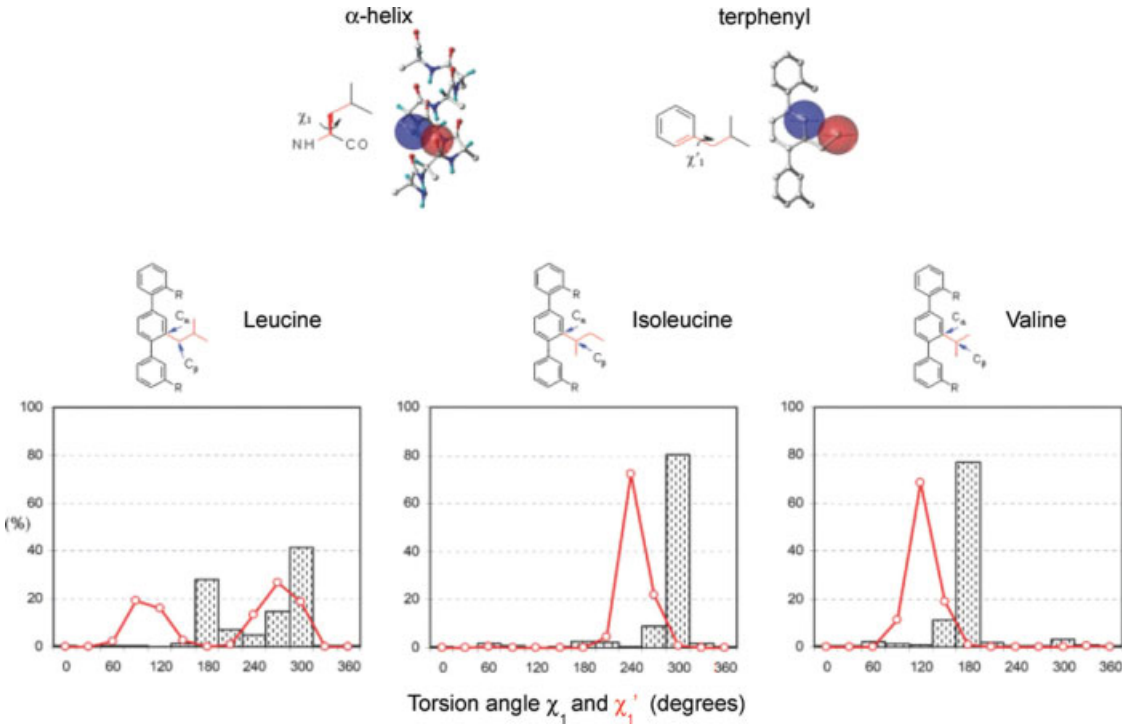

FIGURE 11 There is a fundamental problem[60] with appending amino acid side chain directly to an aromatic ring—the torsion potential of $C_{SP2}—C_{SP3}$ bond is distinctly different than that of $C_{SP3}—C_{SP3}$ (corresponds to the Cα—Cβ bond in a peptide). Notice the distribution of rotamers (red) of aromatic side chains versus observed rotamers of leucine, isoleucine, and valine found in helices in proteins. The offset between red line and hatched bars implies that optimal rotamers observed almost uniquely in helices with isoleucine and valine would be disfavored in aromatic helical mimetics. It is the limitation of rotameric states of the β-branched amino acids such as isoleucine and valine that causes these residues to be less favored entropically when held in a helix.[96]

des,[104,105] organic bicyclic rings such as benzodiazepines,[106] and metal complexes of chiral pentaazacrowns.[107] Arnold et al.[102] used EPL to construct RNase analogs in which synthetic peptide fragments 95–124 were ligated with expressed RNase 1–94. This allowed exploration of the role of the highly conserved Type-VI reverse turn observed in RNase; WUBLAST analysis of genomic sequences of RNAses from 50 species show 49/50 sequences contain a proline at residue 114, the one exception being a leucine found in the capybara (*Hydrochoerus hydrochaeris*) RNase. Residue 113 was a conserved asparagine in most cases, with a few examples of aspartic acid, serine, or lysine substitutions. The question of any selective advantage of preserving this dipeptide reverse turn during the evolution of these different species is intriguing. Residues Asn113-Pro114 located at the end of a β-hairpin were replaced with a reverse-turn peptidomimetic (Figure 13), the dipeptide (*R*)-nipecotic acid–(*S*)-nipecotic acid, shown by Chung et al.,[108] to nucleate reverse-turn segments. The substitution of two exocyclic six-membered rings in the peptide backbone for the single five-membered proline ring and Asn residue was anticipated to enhance the preorganization of

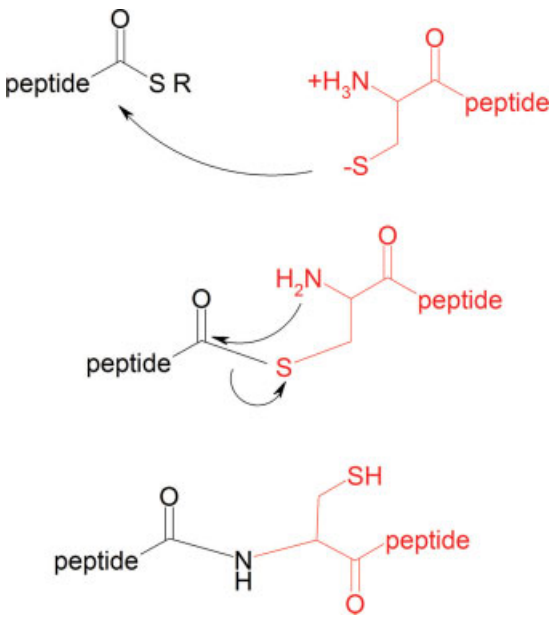

FIGURE 12 Chemical ligation of peptide fragments with unprotected side chains was pioneered independently by two former Merrifield lab members, Steve Kent and James Tam.

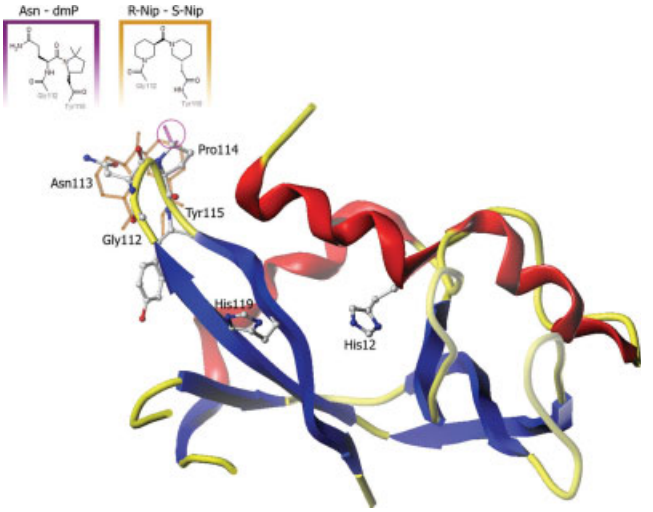

FIGURE 13 RNase A (cartoon representation) has a β-turn at Gly112-Asn113-Pro114-Tyr115 that was chemically modified using expressed protein ligation to generate the chimeric proteins. Both 5,5′-dimethylproline (dmP) substitution for Pro114 and *R*-Nip-*S*-Nip for Asn113-Pro114 have been studied by the Raines group.[116,117] The native β-turn residues are shown in atom-colored CPK representation; the dmP modification (two methyls replacing hydrogens) is shown in magenta, and the *R*-Nip-*S*-Nip modification (two six-membered β-amino acids) is shown in orange.

the unfolded state and, thereby, reduce the entropy of folding. Such a reduction in the entropy of folding should be reflected in a higher melting temperature compared with the wild-type protein.

Torsional Entropy

Estimation of the entropy changes that result from conformational constraints and/or binding to a macromolecule is a topic of considerable interest when attempting to estimate affinities of ligands for receptors.[109] This issue has been extensively studied experimentally by Williams et al.[110–112] and forms the theoretical basis of fragment-based drug discovery,[113] as exemplified in "SAR by NMR."[114] Mammen et al.[115] developed a classical model for estimating the entropy of torsional motion about a single bond. The entropy associated with torsional motion ranges from 0 to 15 J mol^{-1} K^{-1} and varies with the bond length, the hybridization, the symmetry, the sizes of these atoms or groups of atoms, and the extent of conjugation to adjacent bonds. The question of interest, however, is in the actual entropic change introduced by either preorganization of the ligand and/or binding to another molecule as determined experimentally or by computation.

Table I from Arnold et al.[116] is reproduced as part of Table I. Note the three different controls for the native protein (Asn-Pro) and the quantitative agreement in experimental values for both T_m and k_{cat}/K_m. It is clear that the dinipecotic acid substitution at residues 113–114 had little impact, if any, on the enzyme activity, but a measurable, small effect on the melting temperature [ΔT_m by (1.2 ± 0.3)°C, or $\Delta\Delta G_m$ = 2.0 ± 0.4 kJ mol^{-1}].

In a similar study, Arnold et al.[117] introduced 5,5-dimethyl-L-proline (dmP) for Pro114 to stabilize the *cis*-amide bond[118] between residues 113 and 114 by EPL (Figure 13). The catalytic activity k_{cat}/K_m was indistinguishable from that of the native enzyme. The midpoint of the thermal transition for dmP114 RNase was increased, ΔT_m = (2.8 ± 0.3)°C or $\Delta\Delta G_m$ = 4.6 ± 0.4 kJ mol^{-1}. For comparison, replacing Pro114 with glycine or L-alanine causes a very significant decrease in conformational stability ($\Delta T_m = -10$°C, $\Delta\Delta G_m$ = 3.6 kJ mol^{-1}),[119] suggesting an important role of this reverse turn and its associated β-hairpin in stabilizing RNase.

In addition, the rate of protein folding was increased approximately sixfold, as isomerization of the proline *trans*-amide bond was thought to be rate limiting. This is in sharp contrast to the previous study where the introduction of the two nipecotic acid six-membered rings at position 113 and 114 only increased the ΔT_m by (1.2 ± 0.3)°C. RNase has been a focus of protein folding studies by the Scheraga group which have shown multiple folding pathways depending on the redox reagent (DTT versus glutathione)[119,120] or the location of the four disulfide bonds (RNase versus onconase).[119,121] It would be intriguing to analyze the pathways associated with folding of the Pro114dmP mutant. Other proline analogs impact *cis–trans* amide isomerization and, therefore, type-VI reverse-turn formation.[118,122] An excellent geometrical mimic of the *cis*-amide bond, the 1,5-disubstituted tetrazole ring, has been used by Zabrocki and coworkers[123–125] to probe type-VI reverse-turn recognition. Incorporation of a series of such

Table I Impact of 5,5′-Dimethylproline (dmP) Substitution[116] for Pro114 and Dinipecotic Dipeptide (*R*-Nip-*S*-Nip) Turn-Mimetic Substitution[116] for Asn113-Pro114 in RNase on Catalytic Properties (k_{cat}/K_m) and Melting Temperatures (Protein Stability)

Residues 113–114	Origin	T_m (°C)	k_{cat}/K_m ($\times 10^7$ M^{-1} s^{-1})
R-Nip-*S*-Nip	Semisynthesis	64.6 ± 0.2	1.6 ± 0.4
R-Nip-*R*-Nip	Semisynthesis	ND	0.03 ± 0.01
Asn-Pro	Semisynthesis	63.4 ± 0.2	1.5 ± 0.2
Asn-Pro	*E. coli*	63.5 ± 0.1	1.4 ± 0.3
Asn-Pro	Bovine pancreas	63.6 ± 0.2	1.5 ± 0.2
	ΔT_m = (1.2 ± 0.3)°C; $\Delta\Delta G$ = 2.0 ± 0.2 kJ mol^{-1}		
Asn-Ala	$\Delta T_m = -10$°C		
Asn-dmP	Semisynthesis	66.4 ± 0.2	1.6 ± 0.2
Folds 4X Faster	ΔT_m = (2.8 ± 0.3)°C; $\Delta\Delta G$ = 4.6 ± 0.2 kJ mol^{-1}		

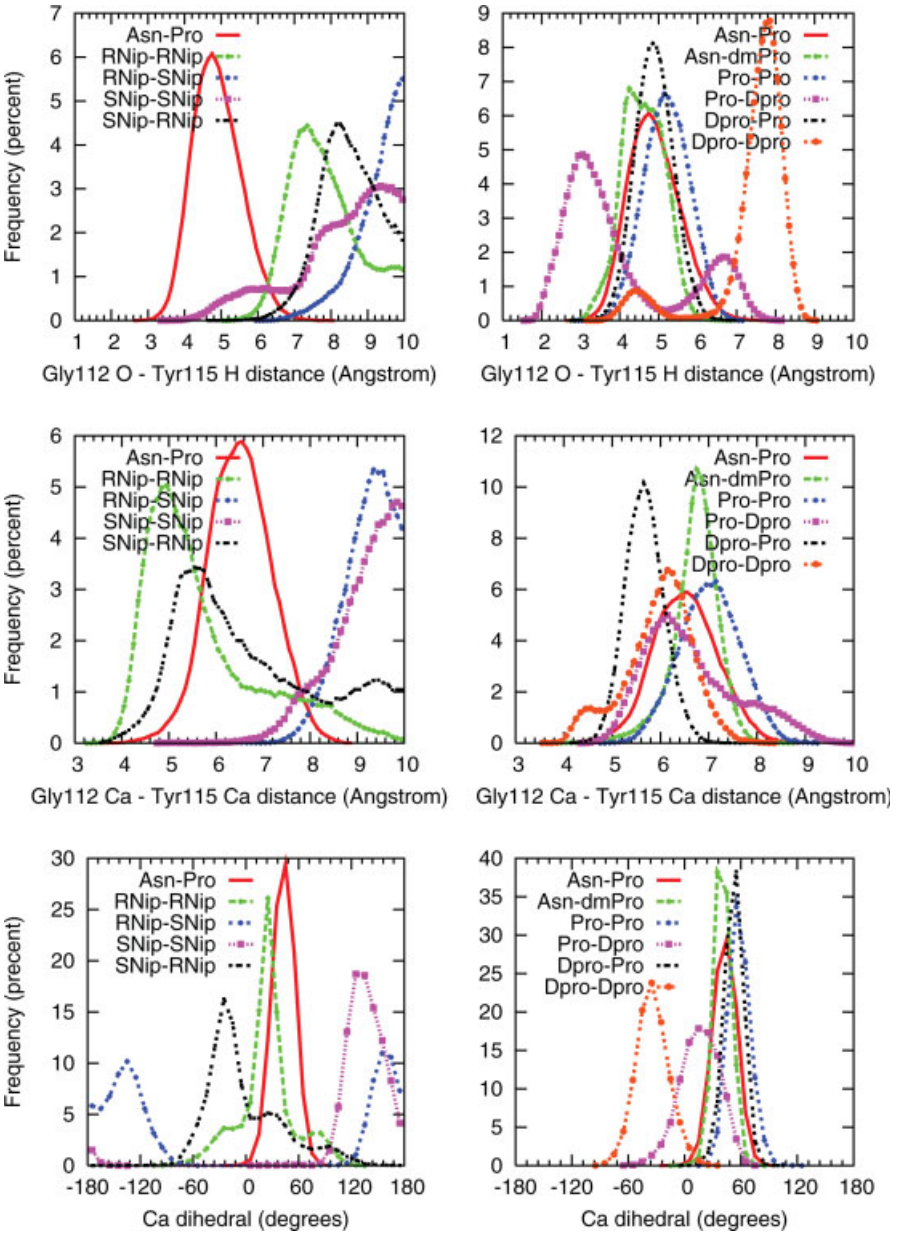

FIGURE 14 Impact of nine reverse-turn mimetics substituted for dipeptide Asn-Pro segment of acetyl-Gly-Asn-Pro-Tyr-NH-methyl (RNase 112–115) on hydrogen bond distances and virtual dihedral-turn metrics based on MD simulations in implicit solvent.

dipeptide analogs to replace Asn113-Pro114 in RNase by EPL with subsequent detailed biophysical studies should provide some insight into the role of this highly conserved dipeptide sequence in RNase function.

MD Simulations of Chimeric RNase

To quantitatively evaluate the relative propensity of reverse-turn mimetics to stabilize β-hairpins, Takeuchi and Marshall[126] monitored various parameters during a MD simulation. For example, the relative time that the distance between the two α-carbons of the first and fourth residue of a capped tetrapeptide containing the mimetic was less than 7 Å was monitored. To investigate the proclivity of the newer reverse-turn mimetics, the native tetrapeptide sequence Gly112-Asn113-Pro114-Tyr115 was capped with acetyl at the N-terminal and with *N*-methyl amide at the C-terminal. Starting with the native sequence, nine mutants with potential reverse-turn mimetics were generated in silico. MacroModel 9.1 was used to run 10-ns MD simulation of the modified peptides in implicit solvent (GB/SA) at 300 K using the

OPLS 2005 force field. The distance between the C-alphas of Gly112 and Tyr115 and the distance between the carbonyl oxygen of Gly112 and amide hydrogen of Tyr115 were recorded (Figure 14) at each time step after initial equilibration similar to the studies by Takeuchi and Marshall[126] on reverse-turn propensity. The virtual dihedral angle defined by the four C-alpha carbons of the reverse turn, as suggested by Tran et al.,[127] of Gly112, Asn113, Pro114, and Tyr115 was also monitored as shown in Figure 14.

The results of the tetrapeptide simulations were quite revealing. In the top two panels of Figure 14, the impact of the nine different dipeptide substitutions on frequency of observation versus distance between the glycine carbonyl oxygen and the tyrosine amide nitrogen (prevalence of a classic hydrogen bond between the i and $i + 3$ residue) are plotted. The middle two graphs of Figure 14 show the frequency versus distance between the α-carbons of glycine and tyrosine, another measure of the propensity to form conformations resembling reverse turns. In native RNase, the distance between the two α-carbons was less than 7 Å over 80% of the simulation; in the *R*-Nip-*S*-Nip chimeric protein, the distance was less than 7 Å for only 1% of the time. While this difference does not directly estimate the amount of preorganization in the unfolded RNase versus the chimeric protein, it does indicate that the introduction of two additional methylenes in the backbone of the hairpin loop by *R*-Nip-*S*-Nip dramatically increases its inherent flexibility and compromises any impact of preorganization of the entropy of folding. In contrast, the use of the reverse-turn nucleators, Pro-D-Pro or D-Pro-Pro, enhanced the reverse-turn potential to equal or greater than native Asn113-Pro114 in the simulations, in accordance with previous estimates of reverse-turn nucleation by Takeuchi and Marshall.[126] It is clear from these graphs that the *R*-Nip-*S*-Nip or *S*-Nip-*R*-Nip dipeptides do not dynamically stabilize the reverse turn seen with Asn-Pro (red line in all graphs) while Asn-dmP, D-Pro-Pro, and Pro-D-Pro mimic and stabilize the reverse-turn as well or better then Asn-Pro itself; in fact, the two bottom graphs of Figure 14, where the virtual dihedral angle between the four α-carbons is shown versus frequency, further confirms stabilization of the reverse turn by these three dipeptides. These graphs can be used to give a crude estimate of the entropic consequences of these dipeptide substitutions. From these results, one would predict that the thermal stability of a chimeric RNase with either Pro-D-Pro or D-Pro-Pro replacing Asn113-Pro114 would be greater than that of the chimeric RNase with *R*-Nip-*S*-Nip. More sophisticated computations using replica exchange are underway to estimate the changes in melting temperature seen for small chimeric proteins in a model system described later.

In further preliminary simulation studies[128] of intact RNase analogs, *R*-Nip-*S*-Nip of Arnold et al.[116] and other potential replacements of Asn113-Pro114 were compared with native RNase. To investigate the minimal effect on the melting temperature [$\Delta T_m = (1.2 \pm 0.3)^\circ$C] observed, the crystal structure of RNase was minimized, the turn mimetic *R*-Nip-*S*-Nip inserted for Asn113-Pro114 and the chimeric structure reminimized. The two additional methylenes of the two β-amino acids were readily incorporated into the structure by simply extending the hairpin loop with nearly identical torsion angles of the rest of the peptide backbone. Thus, little, if any, difference was found between the minimum-energy structures of the two hairpins, suggesting that *R*-Nip-*S*-Nip for Asn-Pro substitution did not disrupt the extended β-sheets of the hairpin, and enthalpic stabilization of the hairpin loop was maintained.

MD Simulations of RNase and RNase S

Nadig et al. did 100-ps simulations of both RNase and RNase S at 300 and 330 K[129] using AMBER 4.0 in TIP3P water. No significant differences in the behavior of the two enzymes was observed, despite the cleavage of the bond between residues 20 and 21 in RNase S that was supposedly responsible for enhanced hydrogen-deuterium exchange and sensitivity to trypsin in the case of RNase S that was previously reported. Differences in sensitivity to trypsin digestion were attributed to the enhanced cleavage of S-protein that had dissociated from RNase S during the experiments, rather than to differences in inherent susceptibility to enzymatic cleavage of RNase and RNase S. A similar argument was applied to hydrogen–deuterium exchange, due to the measured dissociation rate of RNase S of 1.45×10^{-8} M at 15°C.[42] Thus, the presence of small amounts of S-protein and S-peptide during the experimental studies on RNase S can explain the reported enhanced dynamics of RNAse S compared with RNase. It is difficult to imagine that cleavage of the peptide bond between residues 20 and 21 with the resulting changes in the structure of RNase S versus RNase did not impact normal modes and other dynamic properties of the enzyme. One plausible explanation is that the changes in low frequency modes are not sufficiently sampled in the 100-ps simulations.

Dynamics and Enzyme Mechanism

The effect of protein motion on different aspects of enzymatic function and protein complex formation in a variety of systems has become accessible through sophisticated NMR relaxation experiments.[130–138] Alexandrescu et al.[139] determined the ^{15}N backbone dynamics of S-peptide in both its free and bound form. The order parameters derived were used to calculate ^{1}H-^{15}N bond vector entropies that averaged

-12.6 ± 1.4 J mol^{-1} residue K for Thr3-Ser15, the S-peptide residues that became ordered upon binding to S-protein. Further studies[140] of structure/disorder in S-peptide based on NMR residual dipolar couplings indicated that the presence of a native-like α-helix (residues 3–13) undergoing dynamic fraying at either end under experimental conditions that traditionally stabilize helical conformations. These results were entirely consistent with previous studies by Brown and Klee,[141] Kim and Baldwin,[142] and Nelson and Kallenbach[143] that showed that S-peptide had a nascent α-helical segment that could be stabilized by experimental conditions. The dynamics of RNase A itself were later investigated by Cole and Loria[33] by NMR spin-relaxation experiments. RNase A was conformationally rigid on time scales faster than overall rotational tumbling (picoseconds to nanoseconds). The average order parameter, S(2), for RNase A was 0.910 ± 0.051. Twenty-eight of the 124 amino acid residues in RNase underwent chemical exchange on the microsecond-to-millisecond time scale. The microscopic chemical exchange rates, k_{ex}, were quantified by the relaxation-compensated Carr-Purcell-Meiboom-Gill (rcCPMG) experiment for 16 of the 28 residues. The value of k_{ex} was identical for all 16 residues with an average of 1640 s^{-1} and very similar to the RNase k_{cat} value of 1900 s^{-1}. Many of these mobile residues localize to the active site in RNase, including the catalytically crucial amino acids His119 and Asp121. Additional motion was found in the B1, B2, and P0 binding subsites, suggesting possible coupling of motion between the binding and catalytic sites. The activation energy of the motion was measured by applying the rcCPMG experiment at temperatures of 283, 293, and 298 K and was determined to vary between 3.6 and 7.4 kcal mol^{-1}. This activation-energy barrier to conformational motion is very similar to that of the RNase-catalyzed reaction, and thus would not be thermodynamically limiting for catalysis. Correlations of motion and activation energy with enzymatic parameters suggest a possible role for protein flexibility in the molecular enzymatic mechanism of RNase. The data, however, from two modifications of the β-hairpin at residues 113–114 in RNase by EPL yielded identical values of catalytic activity k_{cat}/K_m[116,117] with those of the native enzyme. This is more in concert with the experimental data of Park and Raines[2] that substrate association is the rate-limiting step for RNase. Marcus rate theory suggests that efficient catalysis minimizes the energetics of reorganization,[144] and the correlations in protein dynamics in RNase with enzymatic rates may be misleading. Alternatively, the dynamics of the β-hairpin centered at residues 113–114 may not couple to the active site in RNase. The role of the Asn-Pro reverse turn and β-hairpin centered at residues 113–114 in RNase remains a mystery, as it is highly conserved in different species. As additional motion was observed by NMR in the phosphate (PO)-binding site by Cole and Loria,[33] similar experiments on the K7H/R10H/H12K/H119Q mutant of Moussaoui et al.[145] (discussed later) where the catalytic site now resides at the PO-binding site could be instructive.

ENGINEERING OF CHIMERIC PROTEINS

Mirror-Image Enzymes

Bruce was intrigued with the idea of an all-D enantiomer of RNase. "Will a protein of unnatural configuration bind and react with a ligand of unnatural enantiomeric structure in exactly the same way as the natural all-L enzyme reacts with its normal substrate?" was a rhetorical question he asked on page 139 of his autobiography.[19] Bruce started the synthesis of all-D RNase and its enantiomeric substrate, cytosine-1-β-L-ribofuranosyl-1′,3′ cyclic phosphate in his group, but the project was never completed to our knowledge. His influence inspired his former technician, Angela Corigliano, to synthesize all-D S-peptide while in the lab of Irwin Chaiken and to show it would neither inhibit nor activate S-protein.[146] Steve Kent would address this question with the synthesis of all-D HIV-1 protease and an all-D substrate.[147] The results were as anticipated: a mirror-image biological universe is feasible; the mirror-image enzyme was specific for the mirror-image peptide substrate.

Toward Protein Engineering

Active Site Design. By mutation, it has been possible to reengineer proteins,[148,149] i.e. move an active site from one protein to a new scaffold, change the enzymatic mechanism, etc. Recently, Moussaoui et al.[145] changed the phosphate-binding site of RNase into a catalytic site for cleavage of phosphodiester bonds by the double mutant K7H/R10H. Suppression of the normal active site in K7H/R10H/H12K/H119Q shows a clear increase in exonucleolytic activity which can only be attributed to the new active site. K7H/R10H retained 17% relative activity while the activity of K7H/R10H/H12K/H119Q was reduced to 9%. The k_{cat}/K_m ratio was reduced approximately fourfold for each of the two mutant enzymes compared with native RNase.

Chimeric Proteins. Incorporation of nonnatural amino acids and semirigid peptidomimetics provide unique possibilities for designing proteins that adopt a stable predetermined fold, allowing rational protein engineering to become a reality. Bruce Erickson, a Merrifield lab alumnus, pioneered the incorporation of D-proline to nucleate β-turns[150] in the de novo design of proteins,[151] particularly his seminal work

on betabellins[152] started as a collaboration with Richardson et al.[153] Limiting segmental dynamics may be a useful probe of enzyme mechanism and/or specificity, a topic of increased interest. The ability to design proteins with enhanced stability is of commercial interest in the production of super stabile biocatalysts for green chemistry. For example, multiple tons of the proteolytic enzyme subtilisin, engineered to be stable in detergents at alkaline pH and elevated temperatures, are consumed annually in laundry detergents.[154] To be able to experimentally explore such topics with chimeric proteins is a direct outcome of the invention of solid-phase peptide chemistry and a stated objective (see discussion on pages 125–141 on ribonuclease A in his autobiography) of its inventor, R. Bruce Merrifield,[19] as well as a goal of Emil Fisher whose 100th anniversary of the synthesis of a peptide amide bond was recently celebrated in 2006.

By the same principle of preorganization, incorporating semirigid mimetics of α-helices, β-sheets, and reverse turns into a protein would minimize the entropy $\Delta S_{folding}$ lost on folding through preorganization, while retaining the interactive surface features that optimize the favorable enthalpic interactions $\Delta H_{folding}$ in the folded state. Thus, the stability ($\Delta G_{folding}$) of the mutant folded protein was enhanced compared to the wild-type protein. In effect, one could select a particular folded geometry from the manifold of potential folds for a given sequence by forcing the protein to adopt particular secondary-structure elements at the desired locations in the amino-acid sequence. The first examples of incorporation of reverse-turn mimetics with measurement of enhanced stabilities were into the enzymes HIV protease[155] and RNase A.[116] Chimeric proteins should be thermodynamically more stable because their fold space is limited by semirigid mimetics that reduce the entropic penalty upon folding into the desired 3D structure. In addition, semirigid mimetics should promote the rate of protein folding by nucleation.[117] Modular secondary structure mimetics can serve as building blocks in the design of ultrastable, catalytically active chimeric proteins that resist both proteolytic degradation and denaturation by heat, pH, detergents, etc.

MD Simulations of Chimeric Protein, FSD-1. Designing a protein sequence that folds into a desired three-dimensional shape is known as the inverse protein-folding problem. In nature, protein sequences are limited to combinations of the 20 naturally occurring amino acids plus any posttranslational modifications. Computational protein design methods can identify de novo amino acid sequences that can be folded into predefined topologies.[156,157] As a representative example, the 28-residue full sequence design (FSD-1) ββα-protein was computationally designed by Dahiyat and Mayo to form a stable zinc-finger ββα-fold independent of zinc binding.[156] Starting with the backbone coordinates of the zinc-finger protein Zif268, they selected side-chain rotamers to optimize side-chain/side-chain and backbone/side-chain interactions. The designed protein was synthesized and its structure solved by NMR; the resulting structure's overall backbone RMSD was 1.98 Å relative to the computationally designed target. Residues 3–12 were assigned as a β-hairpin, and residues 15–26 were assigned as α-helical, illustrated in Figure 15. FSD-1 was used as a model system for MD simulations of folding and stability for chimeric proteins incorporating helical mimetics.[128]

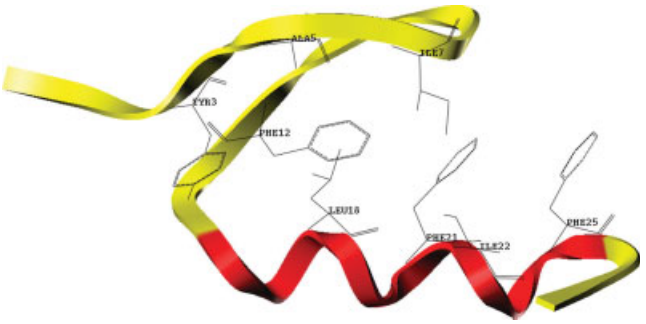

FIGURE 15 Ribbon diagram of FSD-1[156] with helical segment colored red. Side chains contributing to the hydrophobic core area are shown as stick figures. The β-hairpin is shown above the helix, near Ile7.

FSD-1 was chosen as a prototype for chimeric protein engineering because of its small size and because its α-helical segment could be replaced with a semirigid, organic helix mimetic. It should be possible to predict enhanced stability by computational methods due to its small size (28 residues versus 124 residues for RNase). Its short β-hairpin peptide segment could be readily synthesized by solid-phase synthesis and chemically ligated to the organic helical mimetic.[128] Experimental observations and theoretical calculations suggested that helical mimetics based on a triphenyl, tripyridyl, or phenyldipyridyl scaffolds could correctly orient the i, $i + 3$, $i + 4$, and $i + 7$ side chains that formed one side of the surface of an α-helix.[89,92,103] To further investigate the stabilities of helix mimetics, chimeric proteins were designed in silico by ligating four different helix mimetic designs with the β-hairpin subdomain of FSD-1 (Figure 16). A 100-ns MD simulation with GB/SA implicit solvation showed that one of these chimeric proteins was more stable than the native structure and maintained the expected fold during simulations.[128] More detailed simulations using replica exchange at several temperatures are underway to determine if the melting temperatures of the chimeric proteins can be predicted.

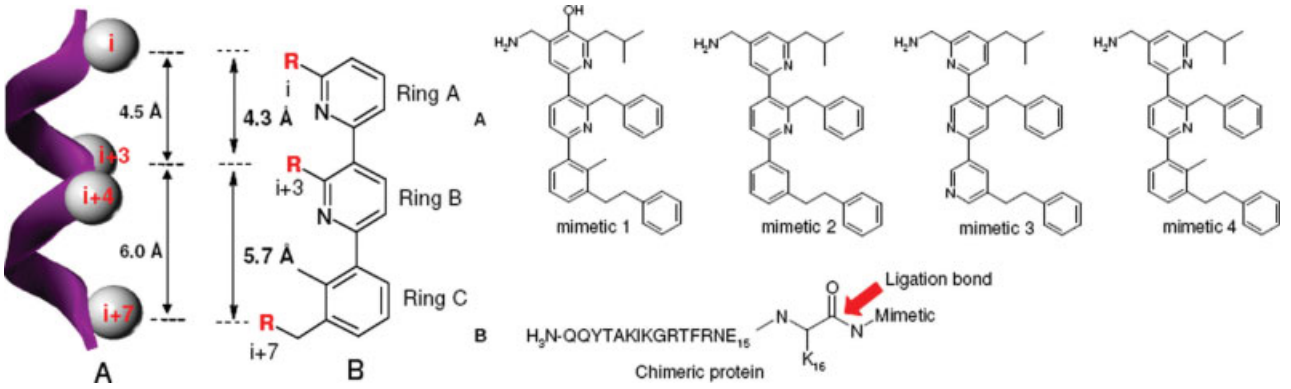

FIGURE 16 Four aromatic helix mimetics bearing Leu18, Phe21, and Phe28 side chains that replaced the helical segment of FSD-1 in chimeric constructs whose stability was estimated by MD simulations with GB/SA implicit solvation.[128] Impact on stability may have been impacted negatively by difference in torsional barriers as shown in Figure 11.[60]

Future Studies of Chimeric RNase Proteins. The extensive experimental database available in the literature[1] on RNase A, RNase S, and the three-component RNase system described in Merrifield's autobiography[19] provides a unique opportunity to dissect many aspects of the thermodynamics of helix recognition, the contributions of entropy to the binding free energy, and the impact of preorganization on protein stability. As these topics require further clarification, several approaches with RNase model systems are of interest. These include measurement of the dynamics of the RNase S chimeric proteins by modern NMR relaxation measurements to determine the impact of preorganization on dynamics and enzyme activity. A direct spectroscopic method to measure the binding entropy of a ligand has recently been developed.[158] In studies on an 11-residue peptide fragment from the C-terminus of the G-alpha subunit of transducin that binds to the photoactivated state of rhodopsin (R*), Kisselev et al. determined the R*-bound conformation of the peptide by transfer NOE experiments.[159] Utilizing an analog of the peptide in which two spin labels had been introduced, Van Eps et al.[158] used pulse EPR to measure the distance between the two nitroxides in the presence of rhodopsin, both dark-adapted and light-activated. In the first case, a distribution of distances between 16 and 36 Å was observed. After irradiation with light, the distribution collapsed to a sharp peak centered at 19 Å, the anticipated distance between the two spin labels based on the R*-bound conformation. The entropy of the peptide in solution and when R* bound can be estimated (see discussion of the configuration partition function, Chapter III in Flory[64]) from the distribution of distances between the two nitroxide labels to give the change in entropy upon peptide binding. The overall change in entropy of the S-peptide/S-protein binding measured by ITC includes the change in entropy of both S-peptide and S-protein, as well as changes in the overall entropy of solvation. Similar studies on spin-labeled S-peptide analogs when free or bound to S-protein would provide an independent experimental estimate of changes in entropy of the peptide analog upon complex formation.

CONCLUSIONS

RNase has proven to be a worthy enzyme of study, as extensive prior investigations have laid the groundwork for more precise experiments to address many questions of current interest. The historical association of this enzyme with the Rockefeller Institute/University had a profound influence on both Bruce Merrifield and his first graduate student (G.R.M.). There is still much to be learnt about the detailed thermodynamics of protein recognition and the impact of preorganization on binding affinity. The role of protein dynamics in enzymatic catalysis by RNase is still an open question that is amenable to detailed analysis by studies on chimeric RNase constructs. Many of the techniques necessary to analyze these issues depended on the development of solid-phase synthesis and the influence that Bruce Merrifield had on the next generation of protein chemists.

The authors acknowledge the overwhelming abundance of literature focused on various aspects of RNase and offer sincere apologies to those investigators whose seminal work was not cited. Computational resources were supported in part by TeraGrid. Prof. Ronald T. Raines of the University of Wisconsin kindly recommended some additional papers to be included after reading an early draft; Profs. Carl Frieden and Jay Ponder, as well as Dr. Christy Taylor of Washington University, kindly read and made suggestions to improve the manuscript. We must finally acknowledge the enormous influence that Bruce Merrifield and the talented colleagues whom he trained at Rockefeller University have had on modern protein chemistry and enzymology. It is indeed a pleasure to stand on the shoulders of such giants of protein biochemistry to glimpse into the future.

REFERENCES

1. Raines, R. T. Chem Rev 1998, 98, 1045–1066.
2. Park, C.; Raines, R. T. Biochemistry 2003, 42, 3509–3518.
3. Anfinsen, C. B. Science 1973, 181, 223–230.
4. Privalov, P. L. Adv Protein Chem 1979, 33, 167–241.
5. Scheraga, H. A.; Konishi, Y.; Ooi, T. Adv Biophys 1984, 18, 21–41.
6. Wedemeyer, W. J.; Welker, E.; Narayan, M.; Scheraga, H. A. Biochemistry 2000, 39, 4207–4216.
7. Leung, H. J.; Xu, G.; Narayan, M.; Scheraga, H. A. J Pept Res 2005, 65, 47–54.
8. Pradeep, L.; Shin, H. C.; Scheraga, H. A. FEBS Lett 2006, 580, 5029–5032.
9. Xu, G.; Narayan, M.; Kurinov, I.; Ripoll, D. R.; Welker, E.; Khalili, M.; Ealick, S. E.; Scheraga, H. A. J Am Chem Soc 2006, 128, 1204–1213.
10. Ribó, M.; Font, J.; Benito, A.; Torrent, J.; Lange, R.; Vilanova, M. Biochim Biophys Acta 2006, 1764, 461–469.
11. Moore, S.; Stein, W. H. Science 1973, 180, 458–464.
12. Dubos, R. J.; Thompson, R. H. S. J Biol Chem 1938, 124, 501–510.
13. Kunitz, M. J Gen Physiol 1940, 24, 15–32.
14. Smyth, D. G.; Stein, W. H.; Moore, S. J Biol Chem 1963, 238, 227–234.
15. Redfield, R. R.; Anfinsen, C. B. J Biol Chem 1956, 221, 385–404.
16. Kresge, N.; Simoni, R. D.; Hill, R. L. J Biol Chem 2005, 280, e47–e48.
17. Gutte, B.; Merrifield, R. B. J Am Chem Soc 1969, 91, 501–502.
18. Gutte, B.; Merrifield, R. B. J Biol Chem 1971, 246, 1922–1941.
19. Merrifield, B. Life During a Golden Age of Peptide Chemistry. American Chemical Society: Washington, DC, 1993; p 297.
20. Thomson, J.; Ratnaparkhi, G. S.; Varadarajan, R.; Sturtevant, J. M.; Richards, F. M. Biochemistry 1994, 33, 8587–8593.
21. Varadarajan, R.; Connelly, P. R.; Sturtevant, J. M.; Richards, F. M. Biochemistry 1992, 31, 1421–1426.
22. Varadarajan, R.; Richards, F. M. Biochemistry 1992, 31, 12315–12327.
23. Richards, F. M.; Vithayathil, P. J. J Biol Chem 1959, 234, 1459–1465.
24. Richards, F. M.; Vithayathil, P. J. Brookhaven Symp Biol 1960, 13, 115–134.
25. Wyckoff, H. W.; Hardman, K. D.; Allewell, N. M.; Inagami, T.; Johnson, L. N.; Richards, F. M. J Biol Chem 1967, 242, 3984–3988.
26. Wyckoff, H. W.; Tsernoglou, D.; Hanson, A. W.; Knox, J. R.; Lee, B.; Richards, F. M. J Biol Chem 1970, 245, 305–328.
27. Hearn, R. P.; Richards, F. M.; Sturtevant, J. M.; Watt, G. D., Biochemistry 1971, 10, 806–817.
28. Finn, F. M.; Hofmann, K. Acc Chem Res 1973, 6, 169–176.
29. Liu, Y.; Hart, P. J.; Schlunegger, M. P.; Eisenberg, D. Proc Natl Acad Sci USA 1998, 95, 3437–3442.
30. Smith, G. P.; Schultz, D. A.; Ladbury, J. E. Gene 1993, 128, 37–42.
31. Finn, F. M.; Dadok, J.; Bothner-By, A. A. Biochemistry 1972, 11, 455–461.
32. Bastos, M.; Pease, J. H.; Wemmer, D. E.; Murphy, K. P.; Connelly, P. R. Proteins 2001, 42, 523–530.
33. Cole, R.; Loria, J. P. Biochemistry 2002, 41, 6072–6081.
34. Chaiken, I. M.; Taylor, H. C.; Ammon, H. L. J Biol Chem 1977, 252, 5599–5601.
35. Dunn, B. M.; Chaiken, I. M. J Mol Biol 1975, 95, 497–511.
36. Taylor, H. C.; Komoriya, A.; Chaiken, I. M. Proc Natl Acad Sci USA 1985, 82, 6423–6426.
37. Kobe, B. Methods Mol Biol 2001, 160, 201–211.
38. Kobe, B.; Deisenhofer, J. J Mol Biol 1996, 264, 1028–1043.
39. Mitchell, J. C.; Kerr, R.; Ten Eyck, L. F. J Mol Graph Model 2001, 19, 325–330, 388–390.
40. Rocchi, R.; Borin, G.; Marchiori, F.; Moroder, L.; Peggion, E.; Scoffone, E.; Crescenzi, V.; Quadrifoglio, F. Biochemistry 1972, 11, 50–57.
41. Connelly, P. R.; Varadarajan, R.; Sturtevant, J. M.; Richards, F. M. Biochemistry 1990, 29, 6108–6114.
42. Varadarajan, R.; Connelly, P. R.; Sturtevant, J. M.; Richards, F. M. Biochemistry 1992, 31, 1421–1426.
43. Graziano, G.; Catanzano, F.; Giancola, C.; Barone, G. Biochemistry 1996, 35, 13386–13392.
44. Ratnaparkhi, G. S.; Awasthi, S. K.; Rani, P.; Balaram, P.; Varadarajan, R. Protein Eng 2000, 13, 697–702.
45. Lin, M. C.; Gutte, B.; Caldi, D. G.; Moore, S.; Merrifield, R. B. J Biol Chem 1972, 247, 4768–4774.
46. Lin, M. C.; Gutte, B.; Moore, S.; Merrifield, R. B. J Biol Chem 1970, 245, 5169–5170.
47. Hodges, R. S.; Merrifield, R. B. Int J Pept Protein Res 1974, 6, 397–405.
48. Hodges, R. S.; Merrifield, R. B. J Biol Chem 1975, 250, 1231–1241.
49. Crestfield, A. M.; Stein, W. H.; Moore, S. Arch Biochem Biophys 1962, 1(Suppl.), 217–222.
50. Libonati, M.; Gotte, G. Biochem J 2004, 380(Part 2), 311–327.
51. Liu, Y.; Gotte, G.; Libonati, M.; Eisenberg, D. Protein Sci 2002, 11, 371–380.
52. Lopez-Alonso, J. P.; Bruix, M.; Font, J.; Ribó, M.; Vilanova, M.; Rico, M.; Gotte, G.; Libonati, M.; Gonzalez, C.; Laurents, D. V. J Biol Chem 2006, 281, 9400–9406.
53. Dyer, K. D.; Rosenberg, H. F. Mol Divers 2006, 10, 585–597.
54. Cho, S.; Beintema, J. J.; Zhang, J. Genomics 2005, 85, 208–220.
55. Smith, G. P.; Schultz, D. A.; Ladbury, J. E. Gene 1993, 128, 37–42.
56. Dickson, K. A.; Haigis, M. C.; Raines, R. T. Prog Nucleic Acid Res Mol Biol 2005, 80, 349–374.
57. Rutkoski, T. J.; Kurten, E. L.; Mitchell, J. C.; Raines, R. T. J Mol Biol 2005, 354, 41–54.
58. Neumann, U.; Hofsteenge, J. Protein Sci 1994, 3, 248–256.
59. Smith, B. D.; Raines, R. T. J Mol Biol 2006, 362, 459–478.
60. Che, Y.; Brooks, B. R.; Marshall, G. R. Protein recognition motifs: design of peptidomimetics of helix surfaces. Biopolymers 2007, 86, 288–297.
61. Kuster, D. J.; Urahata, S.; Ponder, J. W.; Marshall, G. R. In Abstracts of the 51st Biophysical Society Meeting. The Biophysical Society: Baltimore, MD, 2007; Poster 1791.
62. Grossfield, A.; Ren, P.; Ponder, J. W. J Am Chem Soc 2003, 125, 15671–15682.
63. Marshall, G. R.; Bosshard, H. E. Circ Res 1972, 31(Suppl. 2), II-l43–II-l50.
64. Flory, P. J. Statistical Mechanics of Chain Molecules. Hanser: Munich, 1989; 432p.
65. Marshall, G. R.; Hodgkin, E. E.; Langs, D. A.; Smith, G. D.; Zabrocki, J.; Leplawy, M. T. Proc Natl Acad Sci USA 1990, 87, 487–491.

66. Smythe, M. L.; Huston, S.; Marshall, G. R. J Am Chem Soc 1993, 115, 11594–11595.
67. Smythe, M. L.; Huston, S. E.; Marshall, G. R. J Am Chem Soc 1995, 117, 5445–5452.
68. Smythe, M. L.; Nakaie, C. R.; Marshall, G. R. J Am Chem Soc 1995, 117, 10555–10562.
69. Huston, S. E.; Marshall, G. R. Biopolymers 1994, 34, 75–90.
70. Karle, I. L.; Flippen-Anderson, J. L.; Uma, K.; Balaram, P. Proteins 1990, 7, 62–73.
71. Karle, I. L. Biopolymers 2001, 60, 351–365.
72. Toniolo, C.; Crisma, M.; Formaggio, F.; Valle, G.; Cavicchioni, G.; Precigoux, G.; Aubry, A.; Kamphuis, J. Biopolymers 1993, 33, 1061–1072.
73. Lancelot, N.; Elbayed, K.; Raya, J.; Piotto, M.; Briand, J. P.; Formaggio, F.; Toniolo, C.; Bianco, A. Chemistry 2003, 9, 1317–1323.
74. McNulty, J. C.; Silapie, J. L.; Carnevali, M.; Farrar, C. T.; Griffin, R. G.; Formaggio, F.; Crisma, M.; Toniolo, C.; Millhauser, G. L. Biopolymers 2000, 55, 479–485.
75. Barazza, A.; Wittelsberger, A.; Fiori, N.; Schievano, E.; Mammi, S.; Toniolo, C.; Alexander, J. M.; Rosenblatt, M.; Peggion, E.; Chorev, M. J Pept Res 2005, 65, 23–35.
76. Walensky, L. D.; Kung, A. L.; Escher, I.; Malia, T. J.; Barbuto, S.; Wright, R. D.; Wagner, G.; Verdine, G. L.; Korsmeyer, S. J. Science 2004, 305, 1466–1470.
77. Taylor, J. W. Biopolymers 2002, 66, 49–75.
78. Kataoka, T.; Beusen, D. D.; Clark, J. D.; Yodo, M.; Marshall, G. R. Biopolymers 1992, 32, 1519–1533.
79. Shepherd, N. E.; Hoang, H. N.; Desai, V. S.; Letouze, E.; Young, P. R.; Fairlie, D. P. J Am Chem Soc 2006, 128, 13284–13289.
80. Turk, J.; Marshall, G. R. Biochemistry 1975, 14, 2631–2635.
81. Turk, J.; Needleman, P.; Marshall, G. R. J Med Chem 1975, 18, 1139–1142.
82. Turk, J.; Needleman, P.; Marshall, G. R. Mol Pharmacol 1976, 12, 217–224.
83. Turk, J.; Panse, G. T.; Marshall, G. R. J Org Chem 1975, 40, 953–955.
84. Leavitt, S.; Freire, E. Curr Opin Struct Biol 2001, 11, 560–566.
85. Luque, I.; Freire, E. Proteins 2002, 49, 181–190.
86. Jacoby, E. Bioorg Med Chem Lett 2002, 12, 891–893.
87. Orner, B. P.; Ernst, J. T.; Hamilton, A. D. J Am Chem Soc 2001, 123, 5382–5383.
88. Ernst, J. T.; Becerril, J.; Park, H. S.; Yin, H.; Hamilton, A. D. Angew Chem Int Ed Engl 2003, 42, 535–539.
89. Yin, H.; Lee, G. I.; Sedey, K. A.; Kutzki, O.; Park, H. S.; Orner, B. P.; Ernst, J. T.; Wang, H. G.; Sebti, S. M.; Hamilton, A. D. J Am Chem Soc 2005, 127, 10191–10196.
90. Chen, L.; Yin, H.; Farooqi, B.; Sebti, S.; Hamilton, A. D.; Chen, J. Mol Cancer Ther 2005, 4, 1019–1025.
91. VanCompernolle, S. E.; Wiznycia, A. V.; Rush, J. R.; Dhanasekaran, M.; Baures, P. W.; Todd, S. C. Virology 2003, 314, 371–380.
92. Davis, J. M.; Truong, A.; Hamilton, A. D. Org Lett 2005, 7, 5405–5408.
93. Ernst, J. T.; Kutzki, O.; Debnath, A. K.; Jiang, S.; Lu, H.; Hamilton, A. D. Angew Chem Int Ed Engl 2002, 41, 278–281.
94. Kutzki, O.; Park, H. S.; Ernst, J. T.; Orner, B. P.; Yin, H.; Hamilton, A. D. J Am Chem Soc 2002, 124, 11838–11839.
95. Chen, L.; Yin, H.; Farooqi, B.; Sebti, S.; Hamilton, A. D.; Chen, J. Mol Cancer Ther 2005, 4, 1019–1025.
96. Creamer, T. P.; Rose, G. D. Proc Natl Acad Sci USA 1992, 89, 5937–5941.
97. Paulus, H. Annu Rev Biochem 2000, 69, 447–496.
98. Anderson, L. L.; Marshall, G. R.; Baranski, T. J. Protein Pept Lett 2005, 12, 783–787.
99. Anderson, L. L.; Marshall, G. R.; Crocker, E.; Smith, S. O.; Baranski, T. J. J Biol Chem 2005, 280, 31019–31026.
100. Muralidharan, V.; Muir, T. W. Nat Methods 2006, 3, 429–438.
101. Evans, T. C., Jr.; Benner, J.; Xu, M. Q. Protein Sci 1998, 7, 2256–2264.
102. Arnold, U.; Hinderaker, M. P.; Raines, R. T. ScientificWorldJournal 2002, 2, 1823–1827.
103. Che, Y.; Brooks, B. R.; Marshall, G. R. J Comput-Aided Mol Des 2006, 20, 109–130.
104. Haubner, R.; Finsinger, D.; Kessler, H. Angew Chem Int Ed Engl 1997, 36, 1374–1389.
105. Glenn, M. P.; Kelso, M. J.; Tyndall, J. D.; Fairlie, D. P. J Am Chem Soc 2003, 125, 640–641.
106. Hata, M.; Marshall, G. R. J Comput Aided Mol Des 2006, 20, 321–331.
107. Che, Y.; Brooks, B. R.; Riley, D. P.; Reaka, A. J. H.; Marshall, G. R. Chem Biol Drug Des, in press.
108. Chung, Y. J.; Huck, B. R.; Christianson, L. A.; Stanger, H. E.; Krauthauser, S.; Powell, D. R.; Gellman, S. H. J Am Chem Soc 2000, 122, 3995–4004.
109. Marshall, G. R.; Arimoto, R.; Ragno, R.; Head, R. D. Abstr Pap Am Chem Soc 2000, 219, 056–COMP.
110. Williams, D. H.; Davies, N. L.; Koivisto, J. J. J Am Chem Soc 2004, 126, 14267–14272.
111. Williams, D. H.; O'Brien, D. P.; Sandercock, A. M.; Stephens, E. J Mol Biol 2004, 340, 373–383.
112. Williams, D. H.; Stephens, E.; O'Brien, D. P.; Zhou, M. Angew Chem Int Ed Engl 2004, 43, 6596–6616.
113. Murray, C. W.; Verdonk, M. L. J Comput Aided Mol Des 2002, 16, 741–753.
114. Shuker, S. B.; Hajduk, P. J.; Meadows, R. P.; Fesik, S. W. Science 1996, 274, 1531–1534.
115. Mammen, M.; Shakhnovich, E. I.; Whitesides, G. M. J Org Chem 1998, 63, 3168–3175.
116. Arnold, U.; Hinderaker, M. P.; Nilsson, B. L.; Huck, B. R.; Gellman, S. H.; Raines, R. T. J Am Chem Soc 2002, 124, 8522–8523.
117. Arnold, U.; Hinderaker, M. P.; Koditz, J.; Golbik, R.; Ulbrich-Hofmann, R.; Raines, R. T. J Am Chem Soc 2003, 125, 7500–7501.
118. Che, Y.; Marshall, G. R. Biopolymers 2006, 81, 392–406.
119. Schultz, L. W.; Hargraves, S. R.; Klink, T. A.; Raines, R. T. Protein Sci 1998, 7, 1620–1625.
120. Scheraga, H. A.; Wedemeyer, W. J.; Welker, E. Methods Enzymol 2001, 341, 189–221.
121. Xu, X.; Rothwarf, D. M.; Scheraga, H. A. Biochemistry 1996, 35, 6406–6417.
122. Che, Y.; Marshall, G. R. J Org Chem 2004, 69, 9030–9042.
123. Smith, G. D.; Zabrocki, J.; Flak, T. A.; Marshall, G. R. Int J Pept Protein Res 1991, 37, 191–197.
124. Beusen, D. D.; Zabrocki, J.; Slomczynska, U.; Head, R. D.; Kao, J. L.; Marshall, G. R. Biopolymers 1995, 36, 181–200.
125. Nachman, R. J.; Zabrocki, J.; Olczak, J.; Williams, H. J.; Moyna, G.; Ian Scott, A.; Coast, G. M. Peptides 2002, 23, 709–716.

126. Takeuchi, Y.; Marshall, G. R. J Am Chem Soc 1998, 120, 5363–5372.
127. Tran, T. T.; McKie, J.; Meutermans, W. D.; Bourne, G. T.; Andrews, P. R.; Smythe, M. L. J Comput Aided Mol Des 2005, 19, 551–566.
128. Feng, J.; Tessler, L. A.; Marshall, G. R. Int J Pept Res Ther, in press.
129. Nadig, G.; Ratnaparkhi, G. S.; Varadarajan, R.; Vishveshwara, S. Protein Sci 1996, 5, 2104–2114.
130. Eisenmesser, E. Z.; Bosco, D. A.; Akke, M.; Kern, D. Science 2002, 295, 1520–1523.
131. Kern, D.; Eisenmesser, E. Z.; Wolf-Watz, M. Methods Enzymol 2005, 394, 507–524.
132. Eisenmesser, E. Z.; Millet, O.; Labeikovsky, W.; Korzhnev, D. M.; Wolf-Watz, M.; Bosco, D. A.; Skalicky, J. J.; Kay, L. E.; Kern, D. Nature 2005, 438, 117–121.
133. Case, D. A. Acc Chem Res 2002, 35, 325–331.
134. Kay, L. E. J Magn Reson 2005, 173, 193–207.
135. Boehr, D. D.; McElheny, D.; Dyson, H. J.; Wright, P. E. Science 2006, 313, 1638–1642.
136. Clore, G. M.; Schwieters, C. D. J Mol Biol 2006, 355, 879–886.
137. Frederick, K. K.; Kranz, J. K.; Wand, A. J. Biochemistry 2006, 45, 9841–9848.
138. Koglin, A.; Mofid, M. R.; Lohr, F.; Schafer, B.; Rogov, V. V.; Blum, M. M.; Mittag, T.; Marahiel, M. A.; Bernhard, F.; Dotsch, V. Science 2006, 312, 273–276.
139. Alexandrescu, A. T.; Rathgeb-Szabo, K.; Rumpel, K.; Jahnke, W.; Schulthess, T.; Kammerer, R. A. Protein Sci 1998, 7, 389–402.
140. Alexandrescu, A. T.; Kammerer, R. A. Protein Sci 2003, 12, 2132–2140.
141. Brown, J. E.; Klee, W. A. Biochemistry 1971, 10, 470–476.
142. Kim, P. S.; Baldwin, R. L. Nature 1984, 307, 329–334.
143. Nelson, J. W.; Kallenbach, N. R. Biochemistry 1989, 28, 5256–5261.
144. Marcus, R. A. J Chem Phys 2006, 125, 194504.
145. Moussaoui, M.; Cuchillo, C. M.; Nogues, M. V. Protein Sci 2007, 16, 99–109.
146. Corigliano-Murphy, M. A.; Xun, L. A.; Ponnamperuma, C.; Dalzoppo, D.; Fontana, A.; Kanmera, T.; Chaiken, I. M. Int J Pept Protein Res 1985, 25, 225–231.
147. Milton, R. C.; Milton, S. C.; Kent, S. B. Science 1992, 256, 1445–1448.
148. Hellinga, H. W. Nat Struct Biol 1998, 5, 525–527.
149. Dwyer, M. A.; Looger, L. L.; Hellinga, H. W. Science 2004, 304, 1967–1971.
150. Yan, Y.; Tropsha, A.; Hermans, J.; Erickson, B. W. Proc Natl Acad Sci USA 1993, 90, 7898–7902.
151. Engel, M.; Williams, R. W.; Erickson, B. W. Biochemistry 1991, 30, 3161–3169.
152. Lim, A.; Makhov, A. M.; Saderholm, M. J.; Griffith, J. D.; Erickson, B. W. Biochem Biophys Res Commun 1999, 264, 498–504.
153. Richardson, J. S.; Richardson, D. C.; Tweedy, N. B.; Gernert, K. M.; Quinn, T. P.; Hecht, M. H.; Erickson, B. W.; Yan, Y.; McClain, R. D.; Donlan, M. E. Biophys J 1992, 63, 1185–1209.
154. Gupta, R.; Beg, Q. K.; Lorenz, P. Appl Microbiol Biotechnol 2002, 59, 15–32.
155. Baca, M.; Alewood, P. F.; Kent, S. B. Protein Sci 1993, 2, 1085–1091.
156. Dahiyat, B. I.; Mayo, S. L. Science 1997, 278, 82–87.
157. Kuhlman, B.; Dantas, G.; Ireton, G. C.; Varani, G.; Stoddard, B. L.; Baker, D. Science 2003, 302, 1364–1368.
158. Van Eps, N.; Anderson, L.; Hubbell, W. L.; Marshall, G. R. Proc Natl Acad Sci USA, submitted.
159. Kisselev, O. G.; Kao, J.; Ponder, J. W.; Fann, Y. C.; Gautam, N.; Marshall, G. R. Proc Natl Acad Sci USA 1998, 95, 4270–4275.